Biochimica et Biophysica Acta 1818 (2012) 915–924

Contents lists available at SciVerse ScienceDirect

Biochimica et Biophysica Acta

journal homepage: www.elsevier.com/locate/bbamem

Influence of stearyl and trifluoromethylquinoline modifications of the cell penetrating peptide TP10 on its interaction with a lipid membrane

Maja Anko [a], Janja Majhenc [b], Ksenija Kogej [c], Rannard Sillard [d], Ülo Langel [d], Gregor Anderluh [e,*], Matjaž Zorko [a]

[a] Institute of Biochemistry, Faculty of Medicine, University of Ljubljana, Vrazov trg 2, SI-1000 Ljubljana, Slovenia
[b] Institute of Biophysics, Faculty of Medicine, University of Ljubljana, Lipičeva 2, SI-1000 Ljubljana, Slovenia
[c] Chair of Physical Chemistry, Faculty of Chemistry and Chemical Technology, University of Ljubljana, Snežniška 5, SI-1000 Ljubljana, Slovenia
[d] Department of Neurochemistry, Stockholm University, Svante Arrhenius väg 21A, SE-106 91 Stockholm, Sweden
[e] Department of Biology, Biotechnical Faculty, University of Ljubljana, Večna pot 111, SI-1000 Ljubljana, Slovenia

ARTICLE INFO

Article history:
Received 12 July 2011
Received in revised form 23 December 2011
Accepted 27 December 2011
Available online 4 January 2012

Keywords:
Cell-penetrating peptide
PepFect
Peptide-membrane interaction
Pore
Stearylation

ABSTRACT

The PepFect family of cell-penetrating peptides (CPPs) was designed to improve the delivery of nucleic acids across plasma membranes. We present here a comparative study of two members of the family, PepFect3 (PF3) and PepFect6 (PF6), together with their parental CPP transportan-10 (TP10), and their interactions with lipid membranes. We show that the addition of a stearyl moiety to TP10 increases the amphipathicity of these molecules and their ability to insert into a lipid monolayer composed of zwitterionic phospholipids. The addition of negatively charged phospholipids into the monolayer results in decreased binding and insertion of the stearylated peptides, indicating modification in the balance of hydrophobic *versus* electrostatic interactions of peptides with lipid bilayer, thus revealing some clues for the selective interaction of these CPPs with different lipids. The trifluoromethylquinoline moieties, in PF6 make no significant contribution to membrane binding and insertion. TP10 actively introduces pores into the bilayers of large and giant unilamellar vesicles, while PF3 and PF6 do so only at higher concentrations. This is consistent with the lower toxicity of PF3 and PF6 observed in previous studies.

1. Introduction

Plasmids and oligonucleotides are promising therapeutics for treating genetic diseases *via* gene regulation. One of the main obstacles to their use is limited cell delivery resulting from their large size and hydrophilic nature. To overcome this, many viral and non-viral delivery vectors have been developed in recent years. Cell-penetrating peptides (CPPs) constitute a class of highly effective, non-viral vectors [1]. The definition of CPPs has changed over the years, but they are now considered as short peptides of less than 30 amino acids that are able to enter cell membranes and translocate different cargoes into the cells. Their most common features are a positive net charge and amphipathicity [2].

The effectiveness of CPPs is clearly established, however, the mechanism of their entry is still widely debated. CPP mediated transport into the cell is held to occur either as a consequence of direct cell membrane penetration by the CPP or *via* the endocytotic pathway, which is the most common mode when CPP-cargo complexes are used [3–5]. The major concern is that the second, endocytic mode of entry can lead to endosomal entrapment, which seriously reduces the bioavailability of the cargo [6]. With oligonucleotides being the cargo of CPPs, it is necessary for the complexes to reach targets in the cytosol when the cargo is siRNA, or the nucleus when the cargo is a splice-correcting oligonucleotide. *In vitro* experiments have used chloroquine or sucrose to disrupt the endosomal membrane [7]. *In vivo*, different strategies have been employed to enhance therapeutic effectiveness. One is to modify CPPs with chloroquine derivatives to make them more effective at low pH and to destabilize the endosomal membrane [8,9].

We report a study of two chemically modified CPPs from the PepFect family, PepFect3 (PF3) and PepFect6 (PF6) whose structure is based on that of transportan-10 (TP10) [10–12] (Fig. 1). PF3 is N-terminally stearylated TP10. It is known that acylation of peptides by

Abbreviations: CMC, critical micelle concentration; CPP, cell-penetrating peptide; DCM, dichloromethane; DIEA, diisopropylethylamine; DLS, dynamic light scattering; DMF, dimethyl formamide; GUV, giant unilamellar vesicle; LUV, large unilamellar vesicle; MIP, maximum insertion pressure; MLV, multilamellar vesicle; PF, PepFect; POPC, 1-palmitoyl-2-oleoyl-sn-glycero-3-phosphocholine; POPG, 1palmitoyl-2-oleoyl-sn-glycero-3-phospho-(1′-rac-glicerol); QN, N-(2-aminoethyl)-N-methyl-N′-[7(trifluoromethyl)-quinolin-4-yl]ethane-1,2-diamine; Rh, hydrodynamic radius; RT-HPLC, reversed-phase high-performance liquid chromatography; SPR, surface plasmon resonance; SUV, small unilamellar vesicle; TP10, transportan-10

* Corresponding author at: National Institute of Chemistry, Hajdrihova 19, SI-1000 Ljubljana, Slovenia. Tel.: +386 1 320 33 97; fax: +386 1 257 33 90.
E-mail addresses: gregor.anderluh@bf.uni-lj.si, gregor.anderluh@ki.si (G. Anderluh).

0005-2736/$ – see front matter © 2012 Elsevier B.V. All rights reserved.
doi:10.1016/j.bbamem.2011.12.028

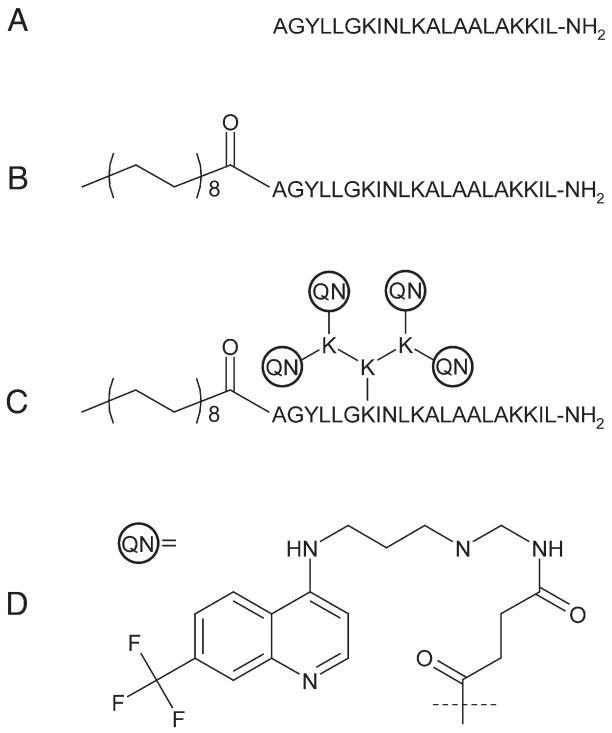

Fig. 1. Chemical structures of TP10 backbone (A), PepFect3 (B), PepFect6 with four trifluoromethylquinoline base derivatives *via* a succinylated lysine tree (C) and a succinylated trifluoromethylquinoline base derivative (D).

fatty acid might increase the ability of peptides for cell internalization; some acylated peptides were able to penetrate cell membrane and enter the cells even if this was not the case for their non-acylated analogs [13]. However, stearylation cannot be regarded as a generally beneficent modification leading to the improved cell-penetration of peptides, since it was shown that it did not increase cell-penetrating efficiency of CPPs penetratin and nona-arginine [10]. In the case of TP10, stearylation leading to PF3 results in substantial increase of the uptake of CPP-oligonucleotide complexes and, as a consequence, splice-correction. The effectiveness of transfection was found to be comparable to that for cationic lipid Lipofectamine 2000™ [10]. The structure of PF6 is based on that for PF3 with the addition of covalently linked, titratable, trifluoromethylquinoline moieties (Fig. 1C and D) [14]. Trifluoromethylquinoline is an analog of chloroquine which is the lysosomotropic agent, inhibiting endosome acidification, leading to endosomal swelling and rupture [15]. As it has been shown, co-incubation of TP10-oligonucleotide complex with quinacrine greatly increased the efficiency of the splice correction by cargo oligonucleotide [10]. Therefore, including the analog of quinacrine into the PF3 structure thus obtaining PF6 seemed a logical development. As a result, in comparison to TP10 and PF3, PF6 is much more potent delivery vector for siRNA *in vitro* and *in vivo*, presumably by trifluoromethylquinoline promoted escape from endosomes by osmotic swelling and thus decreasing endosomal breakdown of CPPs and cargo by delaying endosome acidification [11].

PF6 and probably also PF3, both in complex with cargo, are mainly internalized *via* the endocytic route [11]. This includes interaction with the plasma membrane and then the endosomal membrane to promote passage into the cytoplasm. In this perspective, study of the interactions of PF3 and PF6 with model lipid membranes is needed to better understand the phenomena that occur at the cell and endosome surfaces. Moreover, in order to design and further optimize the PepFect family of delivery vectors, it is necessary to understand the impact of each chemical modification for ability to interact with lipid membranes. Using a combination of biophysical techniques we have compared and evaluated the contributions of the stearyl and trifluoromethylquinoline moieties. The results lead to the conclusion that the stearyl moiety has greater impact on interaction with a lipid membrane, while trifluoromethylquinoline modification has a negligible effect at neutral pH. In comparison with TP10, PF3 and PF6 have greater ability to insert into lipid monolayers composed of zwitterionic phospholipids, but are less potent in inducing leakage of vesicles. The interaction with a membrane composed of negatively charged phospholipids suggests predominantly hydrophobic interactions in the case of PF3 and PF6, while interaction with TP10 is probably governed by electrostatic interactions.

2. Materials and methods

2.1. Reagents

Stearic acid and 2-(1H-benzotriazole-1-yl)-1,1,3,3-tetramethyluronium tetrafluoroborate were from Nova Chemical Company (USA), 1-hydroxybenzotriazole and diisopropylethylamine from Fluka (Sweden). A Discovery® C-18 Supelco® column and α-cyano-4-hydroxycinnamic acid were from Sigma-Aldrich (Sweden). 1-palmitoyl-2-oleoyl-*sn*-glycero-3-phosphocholine (POPC) and 1-palmitoyl-2-oleoyl-*sn*-glycero-3-phospho(1′-rac-glycerol) (POPG) were from Avanti Polar Lipids (USA). TP10 was from Caslo Laboratory (Denmark) and Phospholipid LabAssay™ kit from Wako Pure Chemical Industries, Ltd. (Japan). All other chemicals were from Sigma-Aldrich (Germany) or Merck (Germany).

2.2. Peptide synthesis

2.2.1. Synthesis of PF3

TP10 was synthesized using the t-Boc solid-phase peptide synthesis strategy [16]. PF3 was prepared by treating TP10 peptide resins with 3 equivalents of stearic acid, 3 equivalents of 2-(1H-benzotriazole-1-yl) 1,1,3,3-tetramethyluronium tetrafluoroborate, 3 equivalents of 1-hydroxybenzotriazole and 8 equivalents of diisopropylethylamine in dimethylformamide for 30 min. The product was purified by reversed-phase high-performance liquid chromatography (RP-HPLC) on a Discovery® C-18 Supelco® column using a gradient of acetonitrile/water containing 0.1% TFA. The identity of the purified product was verified by analytical RPHPLC and by Perkin Elmer prOTOF™ 2000 matrix-assisted laser desorption ionization time-of-flight mass-spectrometer (Perkin Elmer, Sweden). The mass spectra were acquired in positive ion reflector mode using α-cyano-4-hydroxycinnamic acid as a matrix (10 mg/mL, 7:3 acetonitrile:water, 0.1% TFA).

2.2.2. Synthesis of the trifluoromethylquinoline derivative

4-Chloro-7-(trifluoromethyl) quinoline (3.8 g, 16.4 mmol) and N-methyl-2,20-diaminodiethylamine (25 mL, 194.1 mmol) were mixed and heated (80 °C, 2.5 h; 130 °C, 3 h; 140 °C, 2.5 h). After cooling to RT, cold dichloromethane (DCM) was added and the precipitate filtered off and discarded. The organic phase was washed (5% $NaHCO_3$ aq×2) and dried [$MgSO_4$(s)], and the solvent removed under reduced pressure, giving N-(2-aminoethyl)-N-methyl-N′-[7-(trifluoromethyl)-quinoline-4-yl]ethane-1,2-diamine (QN) (4.5 g, 14.4 mmol, 83%), calculated mass: 312.3 Da, found: 312.1 Da (Perkin-Elmer prOTOF™ 2000 O-TOF MALDI instrument). The product (>90% purity according to HPLC) was used without further purification.

2.2.3. Synthesis of PF6

Resin-bound TP10 [Fmoc-AGYLLGK(ε-Mtt)INLKALAALAKKIL-Rink amide resin] was treated to generate the N-terminal free amine (35% piperidine, 40 min), followed by coupling of stearic acid, BOP [benzotriazol-1yloxytris(dimethylamino)-phosphonium hexafluorophosphate] and diisopropylethylamine (DIEA) in DCM for 1 h. To

the ε-amino group of Lys^7 (deprotected by repeated washes with 1% TFA, 3–4% TIS in DCM, 1–1.5 h), Fmoc-Lys(Fmoc)-OH (3–5 eq.) was coupled as HOAt (1-hydroxy-7-azabenzotriazole) ester. After Fmoc removal (35% piperidine, 40 min), repeated coupling and final Fmoc removal resulted in a lysine tree containing four free amino groups. These were treated with succinic anhydride (1.5 eq.) and DIEA (3 eq.) in dimethyl formamide (DMF) for 10 min. QN (2.5 eq. in DMF) was coupled overnight to the succinic acid modified lysine tree [TBTU/HOBt (3 eq.) and DIEA (6 eq.)]. After cleavage [water/TIS/TFA 2.5/2.5/95 (v/v)], filtration, precipitation (cold ether) and drying (lyophilization), crude PF6 was obtained. It was purified by RPHPLC, C18 preparative column (5 mm), 45% acetonitrile (ACN)–water [0.1% TFA], 5 min; 45–85% ACN, 60 min, and eluted at 80% ACN. After freeze-drying, purity was >90% (HPLC). The product was analyzed [alphacyano-4-hydroxy-cinnamic acid (α-CHCA) as crystallization matrix] by MALDI MS (Perkin-Elmer prOTOF™ 2000 O-TOF, positive mode); calculated mass: 4408.8 Da, found: 4410.4 Da. The molarity of PF6 and other peptides was determined based on dilutions of accurately weighed substances.

2.3. Critical micelle concentration determination by adsorption at the air/water interface

Adsorption studies were carried out with a Micro Trough S (Kibron Inc., Helsinki) using alloy wire (modification of the Wilhelmy plate method). Small volumes of peptide were added consecutively through a hole connected to the subphase, which consisted of 154 mM NaCl in water. The surface pressure (π) was determined when the thoroughly stirred solution reached equilibrium. The critical micelle concentration (CMC) was determined at the breakpoint when no further increase in surface pressure was observed [17], denoting that the saturation pressure (π_{sat}) was reached.

2.4. Penetration of CPPs into the phospholipid monolayer

Lipids (POPC or POPG) dissolved in chloroform/methanol (3/1, v/v) were spread gently over the subphase (154 mM NaCl in water) in order to obtain a defined initial surface pressure (π_i). After 15 min, when the solvent had evaporated, a small amount of highly concentrated peptide solution was injected through a hole connected to the subphase. The final concentration of CPP was slightly below the CMC [17,18]. The change in surface pressure (Δπ) was recorded as a function of time until a stable signal was obtained. The linear plot of Δπ as a function of π_i was extrapolated to $\Delta\pi = 0$ to give the maximum insertion pressure (MIP), which is a measure of the relative penetrative capacity of a peptide into the monolayer [19].

2.5. Preparation of unilamellar vesicles (small, large and giant)

Phospholipid powder of POPC or a mixture of POPC and POPG at the desired molar ratio was dissolved in chloroform. Solvent was removed by rotary evaporation and subsequent high-vacuum evaporation at 50 mbar for ~4 h to obtain dry lipid film. The lipid film was hydrated with TRIS buffer (140 mM NaCl, 20 mM TRIS, 1 mM EDTA, pH 7.5), or a calcein solution (60 mM calcein in TRIS buffer) for calcein release studies. The mixture was shaken vigorously using a tabletop shaker to obtain multilamellar vesicles (MLVs).

Small unilamellar vesicles (SUVs) were prepared by sonication of MLV dispersion for 30 min with 10 s on and off cycles, using a pulsed sonicator (Vibracell VC 500 Sonics & Materials). Vesicles were then centrifuged at top speed in a benchtop centrifuge to remove particles released from the sonication probe and incubated at 45 °C for 30 min to allow SUV membrane to anneal.

Large Unilamellar Vesicles (LUVs) were prepared by subjecting MLVs to six freeze (liquid nitrogen)–thaw cycles to hydrate the membranes. MLVs were extruded through a 100 nm polycarbonate membrane with a small volume extruder (Avestin, Canada) at room temperature. This yielded unilamellar vesicles with an average diameter of 100 nm as examined by differential light scattering (DLS). The lipid concentration was measured using a Phospholipid LabAssay™ kit.

Giant Unilamellar Vesicles (GUVs) were prepared by electro-formation by the method of Angelova et al. [20], modified by Mally et al. [21]. 12 μL of POPC dissolved in chloroform/methanol (1/1, v/v) was applied on the two platinum electrodes under low pressure to allow for solvent evaporation. The electrodes were then placed into a preparation chamber filled with 0.2 M sucrose solution. Alternating current of frequency 10 Hz and amplitude of 5 V was applied across the electrodes. After 2 h, the frequency was reduced to 5 Hz and the voltage amplitude to 4 V. After 15 min, the frequency and amplitude were decreased to 2.5 Hz and 3 V and, after a further 15 min, finally to 1 Hz and 2 V. The latter conditions were maintained for at least 30 min more to allow the GUVs to detach from the electrodes. Vesicles containing 0.2 M sucrose solution were suspended in iso-osmolar glucose solution to create sugar asymmetry between the inside and the outside of vesicles. Freshly prepared vesicles may have tethers and other protuberances, therefore, we used vesicles at least 1 day old, to allow the membrane to achieve its relaxed state. GUVs were used within 3 days.

2.6. Surface plasmon resonance (SPR)

The interaction of CPPs with lipid monolayer was monitored using a Biacore X analytical system (GE Healthcare) equipped with HPA sensor chip as described [22–24]. The TRIS buffer solution was filtered through a 0.22 μm filter and degassed before each experiment. The sensor chip was installed and the surface cleaned with 300 s injection of non-ionic detergent, 40 mM N-octyl β-D-glucopyranoside, at a flow rate of 5 μL/min. Immediately afterwards, SUVs composed of POPC or a mixture of POPC and POPG at 1 mM lipid concentration were applied for 20 min at 2 μL/min. The so formed lipid monolayer surface was conditioned with an injection of 10 mM NaOH (60 s, 50 μL/min) to obtain a stable baseline. Monolayers prepared in this way served as a model membrane surface to study CPP binding to membrane. Peptide solutions were injected over a lipid surface at a flow rate of 10 μL/min for 3 min. The peptide solution was then replaced by TRIS buffer and the peptide allowed to dissociate from the lipid monolayer for another 3 min. The monolayer with bound peptide was removed completely from the sensor chip by 1 min injections of N-octyl β-D-glucopyranoside and each experiment was performed on a freshly generated lipid monolayer surface.

2.7. Calcein release

LUVs loaded with calcein were prepared as described in Section 2.5. Free calcein was removed from the LUVs by gel filtration on a small G-50 column. Vesicles were stored at 4 °C and used within 2 days. The permeabilization activity of CPPs was measured using a fluorescence microplate reader (Fluostar, SLT, Austria). A 96 well microtiter plate was filled with 200 μL/well of TRIS buffer that contained 20 μM lipids and increasing concentrations of CPPs, and incubated for 30 min at a room temperature. Samples were excited at 485 nm and fluorescence monitored at 538 nm. The maximal fluorescence intensity, corresponding to 100% leakage, was determined by lysing the vesicles with 2 mM Triton X-100. The percentage of permeabilization, R (%), was then calculated according to the following equation:

$$R(\%) = (F - F_0)/(F_{max} - F_0) \times 100.$$

F and F_0 are the values of fluorescence before and after addition of CPPs, and F_{max} the intensity after addition of Triton X-100.

2.8. Dynamic light scattering (DLS)

Particle size analysis was performed using a 3D-DLS Spectrometer from LS Instruments GmbH (Fribourg, Switzerland) equipped with a 20 mW He-Ne laser operating at a wavelength of 632.8 nm [25]. Measurements were performed at a scattering angle of 90° and the intensity correlation functions were analyzed using the Contin software to give the hydrodynamic radius (Rh) of the scattering particles. All measurements were performed at 25 °C in TRIS buffer filtered through filters with a pore size of 0.22 μm. To get an insight into the influence of CPPs on LUV integrity, 1 mL of a 20 μM LUV solution was analyzed by DLS, followed by addition of a small volume of highly concentrated CPP to the LUV suspension to the desired CPP concentration and particle size again analyzed, immediately and after 30 min of incubation, to correlate the results with those on calcein release. The aggregation of CPPs was measured in a similar way in the absence of LUVs.

2.9. Observation of GUVs by phase-contrast microscopy

GUVs appear dark against the background as a consequence of the difference in refractive index of GUV contents (sucrose solution) and the surrounding medium (glucose solution). A white halo, characteristic of a phase-contrast image, appears around the vesicle. Formation of pores by CPPs was followed by exchange of sucrose and glucose across the lipid membrane which results in disappearance of the halo and fading out of GUVs. GUVs were studied singly and as a vesicle population.

2.9.1. Observation of a single GUV

GUVs were observed under an inverted optical microscope (Opton IM35 Zeiss) with phase-contrast objective (40× Ph2 PLAN). The vesicles were monitored using a high resolution camera (CCD-IRIS, Sony) with recording on S-VHS-XP pro TDK tapes. GUVs were transferred one at the time, using a micropipette, into the observation cell filled with an iso-osmolar glucose solution and recorded for 30 min. GUVs were selected based on their unilamellarity, absence of visible protuberances, and size around 50 μm diameter.

2.9.2. Observation of a vesicle population

GUVs were observed under an inverted optical microscope (Nikon Diaphot 200) with phase-contrast objective (20× Ph2/DL) and images were recorded with digital camera (Hamamatsu C4742-95). 20 μL of 0.2 M glucose containing increasing concentrations of peptides was added to 180 μL of GUV solution prepared in 0.2 M glucose. GUVs with the peptides were placed in one observation chamber and GUVs diluted only with glucose were placed in a second observation chamber of the same volume for negative control. Vesicles larger than 20 μm were counted in fifteen observation fields in each chamber after 30 min of incubation. Vesicles that retained their halo effect were regarded as intact and vesicles without halo effect as faded GUVs. The fraction of burst GUVs was calculated from the ratio between the number of GUVs in the presence and absence of CPPs. It should be noted that, when the vesicle is completely faded, it becomes flotant and can be lifted out of the observation field, so some of the faded vesicles could be included in the burst ones.

2.10. Statistical analysis

Statistical analysis (one way ANOVA) was done by using PRISM4 program (GraphPad Software Inc., USA). Statistical relevance was assessed by Tukey's multiple comparison test.

3. Results

3.1. CMC determination by adsorption at the air/water interface

The affinity of CPPs for the air–water interface and their amphipathicity were determined by experiments at the air-water surface. All three peptides showed a clear amphipathic character with high π_{sat}, the highest being observed for PF3 (Fig. 2). The modified CPPs, PF3 and PF6, exhibited distinctly higher π_{sat} values (38.0 ± 0.5 mN/m and 32.7 ± 0.5 mN/m, respectively) than TP10 (24.8 ± 0.4 mN/m), which can be attributed to the presence of the stearyl moiety. One way ANOVA analysis confirmed that π_{sat} values of all three tested CPPs differ significantly ($P<0.001$, $n=3$, Tukey's multiple comparison test). The presence of the trifluoromethylquinoline moieties in PF6 results in a lower amphipathicity, which is reflected in a lower π_{sat} than that of PF3. The CMCs were determined by measuring the difference in surface pressure as a function of peptide concentration, resulting in values of 0.40 ± 0.03, 0.60 ± 0.03 and 0.52 ± 0.04 μM for TP10, PF3 and PF6 (averages ± S.D. of three independent determinations). By one way ANOVA analysis using Tukey's multiple comparison test it was found that CMC of TP10 significantly differ from CMC of PF3 ($p<0.001$, $n=3$) and PF6 ($p<0.05$, $n=3$), while CMCs of PF3 and PF6 are not significantly different ($P>0.05$, $n=3$). Because a value of 38 nM was obtained for TP10 [26], using a slightly different method, we also determined the CMC for the detergent sodium dodecyl sulfate with our experimental setup, as a control. A value of 8 mM was obtained, which agrees well with the values reported in the literature [27].

3.2. Penetration of CPPs into phospholipid monolayers

The affinity of CPPs for phospholipid monolayers was determined from changes in initial surface pressure after the injection of peptides into the subphase. The maximum insertion pressure, MIP, is the value up to which a peptide can insert into the monolayer and beyond which no insertion takes place [28,29]. Using the POPC monolayer the MIP values for TP10, PF3 and PF6 were 34.2 ± 1.6, 49.9 ± 1.2 and 46.5 ± 0.8 mN/m (Fig. 3). This indicates that the strength of interaction for POPC phospholipids follows the order PF3 > PF6 > TP10. Replacing the zwitterionic POPC with the negatively charged POPG monolayer results in a significantly greater MIP for TP10 of 46.8 ± 1.1 mN/m (Fig. 3A), which has been already observed [26]. In contrast, the MIP values for PF3 and PF6 in a POPG monolayer were lower, at 39.9 ± 0.9 and 38.1 ± 0.8 mN/m (Fig. 3B, C).

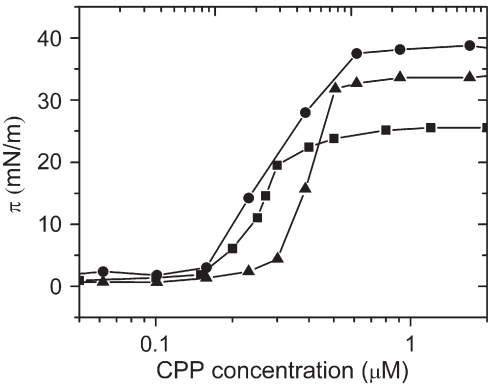

Fig. 2. Affinity of CPPs for an air–water interface. Increase of surface pressure (π) is plotted as a function of CPP concentration in the subphase; TP10 (■), PF3 (●), PF6(▲).

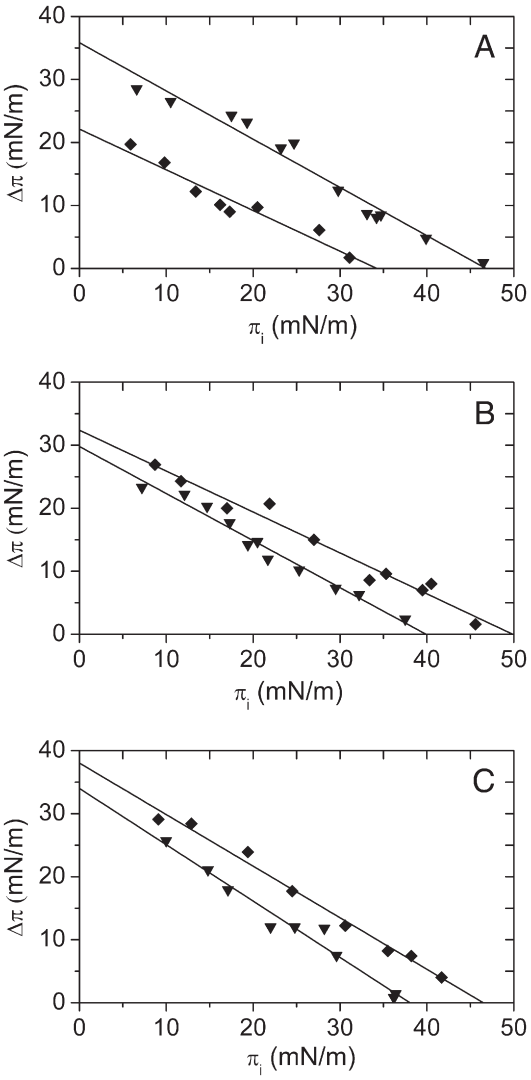

Fig. 3. Penetration of CPPs into phospholipid monolayers measured by the change in surface pressure Δπ. Insertion of (A) TP10, (B) PF3 and (C) PF6 into POPC (▼) and POPG (♦) monolayers.

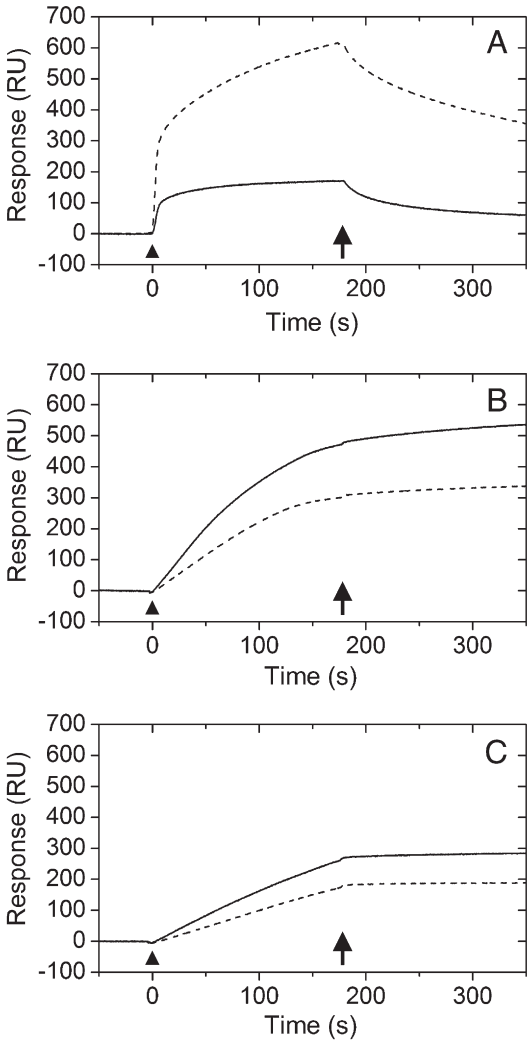

Fig. 4. CPP–lipid monolayer interactions as measured with SPR using an HPA sensor chip. CPPs were injected for 3 min and left to dissociate for another 3 min. Experiments were performed at 25 °C with TRIS as running buffer. Sensograms depict binding of 2.5 μM TP10 (A) and 0.5 μM PF3 (B) and PF6 (C) to POPC (solid line) or POPC:POPG (5:5) monolayers (dashed line). The arrowhead and arrow denote the start of the association and dissociation phases, respectively.

3.3. CPP–lipid monolayer interactions measured by SPR

The interaction of CPPs with lipid membranes was further evaluated using SPR [24]. We initially attempted to use L1 and SA sensor chips, which enable stable immobilization of liposomes *via* lipophilic anchors or liposomes containing biotinylated lipids, respectively [24]. However, CPPs exhibited significant non-specific binding to the sensor chips in the absence of liposomes (data not shown), which precluded peptide membrane interaction analysis. We therefore used an HPA sensor chip that allows formation of a stable lipid monolayer [23]. We immobilized between 1400 and 2300 RU of lipids, which is enough to cover the majority of the flow-cell surface, thus minimizing the non-specific interactions with the hydrophobic alkanethiol-covered surface of the chip [23]. PF3 and PF6 bound considerably to the POPC monolayer (several hundred RU), while binding of TP10 was significantly lower and characterized with high dissociation rate. For example, less than 100 RU remained bound to the monolayer at five times higher concentration in comparison with PF3 or PF6 (Fig. 4). The binding of modified CPPs was characterized by low dissociation (Fig. 4). Interestingly, the signal for modified CPPs increased in the dissociation phase, particularly for PF3 (Fig. 4B), indicating possible peptide-induced reorganization of the lipid monolayer. A decrease in PF3 and PF6 binding was observed when negatively charged POPG was included in the monolayer (Fig. 4). However, the opposite tendency was observed with TP10 which now shows greater affinity for negatively charged lipids. SPR results are thus in accord with the results of the lipid monolayer insertion experiments described above.

3.4. CPP interaction with large unilamellar vesicles

3.4.1. Leakage of entrapped calcein from LUVs

The membrane perforating effect of the peptides was investigated by monitoring calcein release from LUVs composed of POPC and POPC:POPG mixtures. The percentage of leakage induced by CPPs from neutral POPC LUVs is presented in Fig. 5A; leakage induced by 2 mM Triton X-100 was taken as 100%. All three peptides induced leakage at low concentrations and reached high and comparable levels of maximal leakage. TP10 induced 50% leakage at only 0.025 μM concentration and reached a maximal leakage of 82%, while PF3 and PF6 induce 50% leakage at 0.134 and 0.125 μM concentrations and caused maximal leakages of 83% and 70%. TP10 is a very potent inducer of membrane leakage, while stearylation reduces the ability, as observed for PF3 and PF6. The addition of trifluoromethylquinoline moieties does not have a major effect on calcein release, only slightly reducing the maximal leakage. In order to study the

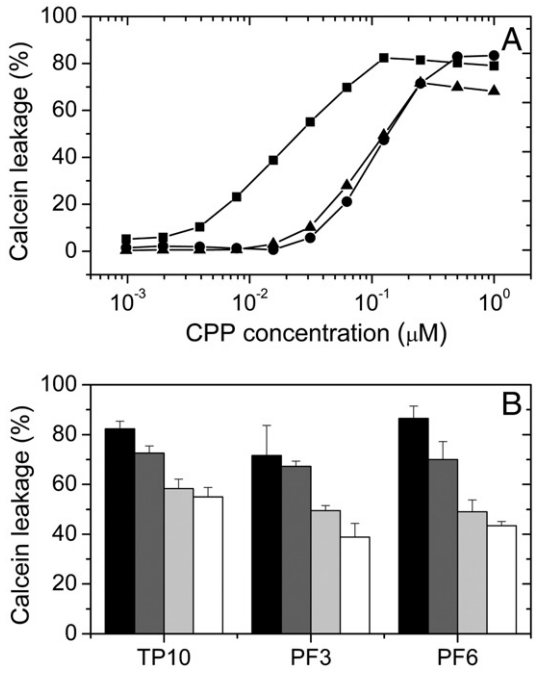

Fig. 5. Calcein leakage from LUVs induced by CPPs. The concentration of lipids was 20 μM. (A) The percentage of calcein leakage from POPC LUVs for TP10 (■), PF3 (●) and PF6 (▲) plotted as a function of peptide concentration. (B) Calcein release from POPC:POPG LUVs at 1 μM concentration. The shift in color from black toward white signifies gradual change in molar composition of POPC:POPG (black bars 10:0, dark gray 9:1, light gray 7:3, white 5:5). The values represent the means and standard deviations for at least three independent experiments.

contribution of negatively charged phospholipids to the ability of CPPs to induce membrane leakage, LUVs with different POPC:POPG molar ratio were tested. For all three CPPs a tendency to reduce calcein release was observed with increase in POPG content (Fig. 5B).

3.4.2. Integrity of LUVs

Dynamic light scattering was employed to examine whether the CPPs affect the integrity of LUVs. Experimental conditions used in this study were the same as for the above leakage study. Rh distribution functions of LUVs were determined before and after the addition of peptides at a final concentration of 1 μM, at which the release of calcein was maximal for all CPPs (Fig. 6). The mean Rh was 50 nm, which corresponds to the diameter of pores in polycarbonate membranes (100 nm) used in the extrusion phase of the preparation process. Addition of TP10 and PF3 does not change either the shape or the position of the distribution function (Fig. 6A, B). Moreover, the intensity of scattered light by LUVs also remains unchanged. This indicates that TP10 and PF3 do not disintegrate the LUVs but release calcein through pore-like structures in the bilayer. This conclusion is further corroborated by the fact that the light scattering intensity decreases to the level of buffer background when Triton X-100, which breaks down LUVs into smaller mixed micelles [30], is added (data not shown). Immediately after the addition of 1 μM PF6 to an LUV suspension the scattered light intensity increased considerably, which is ascribed to aggregates of PF6 (Fig. 6C). Intensity of the LUV peak decreased and remained stable for the following 30 minute incubation (Fig. 6C). At the same time a second peak appeared, with a mean Rh value around 180 nm that increased to 370 nm during incubation. The observed decrease in the LUV peak is thus a consequence of the contribution of this new peak in the distribution, which corresponds to larger particles. To confirm the origin of the second peak the behavior of PF6 without LUV solution was examined. Fig. 6D shows that PF6 forms aggregates with Rh around 130 nm that grow in the course of time. The detected PF6 aggregates in the presence of LUVs are larger and grow faster than those in the absence of LUVs (compare Fig. 6C and D). The reason for this could be the establishment of mixed particles of lipids and PF6 aggregates. Contrary to PF6, pure TP10 and PF3 solutions were observed to scatter light very weakly (data not shown), which shows that these two CPPs do not form larger associated structures. These results indicate that all CPPs are unable to disintegrate LUVs.

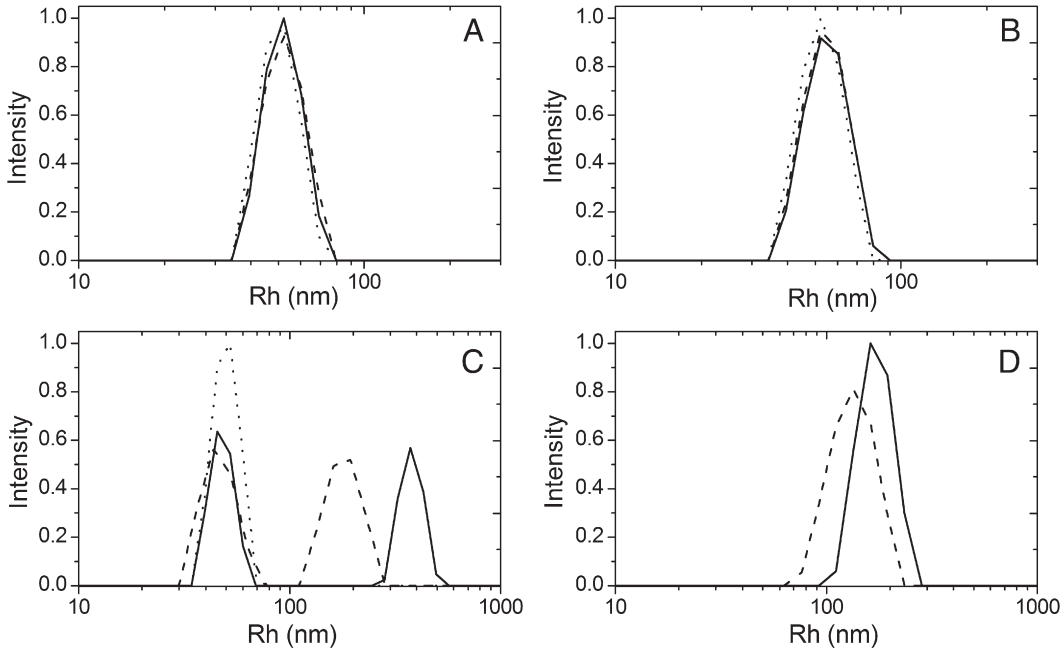

Fig. 6. The normalized hydrodynamic radius (Rh) distribution functions of 20 μM LUVs (dotted line), LUVs with a peptide immediately after addition (dashed line) and LUVs with a peptide after 30 min of incubation (solid line). (A) TP10, (B) PF3 and (C) PF6. (D) Rh size distribution of PF6 aggregates without LUVs.

3.5. CPP interaction with giant unilamellar vesicles

The effect of CPPs on GUVs was evaluated by phase-contrast microscopy, with two different approaches.

3.5.1. Observation of a single GUV

For all three CPPs the observed GUV behavior was classified into three different events. In the lowest concentration range of CPPs (below 0.1 μM) vesicles change their shapes. Initially spherical vesicles become flaccid (Fig. 7A) and fluctuations of the vesicle shapes or formation of tubular structures (Fig. 7B) was repeatedly observed, possibly indicating the intercalation of CPPs into the membrane. The effect could be observed already at concentrations around 0.01 μM and with the increasing intensity in higher concentration. It seemed to be slightly more pronounced with TP10 than with PF3 and PF6 but the quantification of the effect is, however, difficult to assess. Vesicles retained their halo effect during the observation time, indicating that at these concentrations peptides do not cause any perforation of the membrane that allows exchange of outer and inner solutes. At higher peptide concentrations (above 0.1 μM) a decrease of the halo intensity (Fig. 7D) or rapid burst leading to the disruption of vesicles was observed (Fig. 7E). Reduction in halo intensity indicates mixing of the inner and outer solutions as a result of pore formation by CPPs. The process has two phases. First, we observed a longer lag phase (10 to 20 min) without decrease of the halo effect. During this phase the initially flaccid vesicle fills with the solution and become spherical, with stretched membrane. Differences in duration of this phase can be ascribed to the differences in the initial flaccidness of GUVs. The second phase lasted from 2 to 4 min and was seen as a decrease of the halo intensity, accompanied by transient pore [31] openings, as seen in Fig. 7C. At the highest concentration range used (above 2 μM) vesicles also first become spherical, indicating increase in the membrane tension. Subsequently, all vesicles burst and disintegrated in 2 to 4 min after transfer into the CPP solution. Until the final burst, the GUVs appear to maintain their optical contrast due to sugar asymmetry. The observed phenomena are probably a consequence of pore sizes that allow unequal flow of sugars and result in osmotic pressure change. CPPs appear to form pores in the bilayer which preferentially allow influx of glucose which is smaller than sucrose. This results in unequal concentration of solutes inside and outside GUV and drives water in GUV. The increase of osmotic pressure inside the GUVs is compensated by transient tension pore openings which enable a vesicle to eject part of its contents. Transient tension pore can be observed by the microscope (see Fig. 7C) while much smaller pores induced by CPPs are not seen. At higher concentrations of CPP more CPP induced pores are formed, so that osmotic pressure is changed rapidly and cannot be compensated by the opening of transient pores. Consequently, GUVs burst and disintegrate [32].

3.5.2. Observation of a vesicle population

We further evaluated and compared effects of the three CPPs at different concentrations by observing a vesicle population. As with the single GUV approach, the effects were classified into three classes: intact, faded and burst GUVs. The number of burst GUVs was estimated from the ratio of the numbers of GUVs in the presence and absence of CPPs (Fig. 8A, B). Fig. 8C represents fractions of intact, faded and burst GUVs as a function of the CPP concentration. With increasing

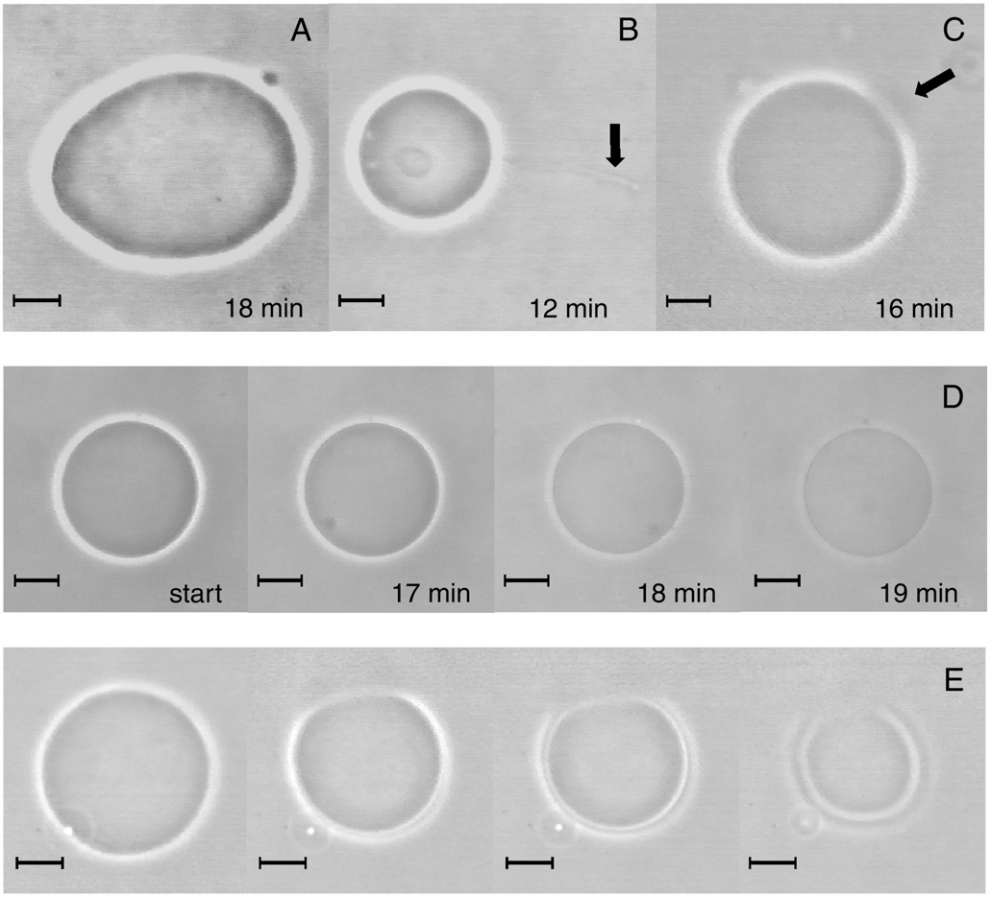

Fig. 7. Effects of CPPs on GUVs as seen by observing a single vesicle by phase contrast microscopy. (A) Shape transformation of GUV in 0.1 μM PF6. (B) Formation of tubular structures (indicated by an arrow) in 0.1 μM PF3. (C) Formation of transient pore (indicated by an arrow) in 0.5 μM TP10. Sequence of images showing time dependence of decreasing halo effect of GUV in 1 μM PF3 (D) and GUV burst in 2 μM PF6 (E). The typical burst is shown. Typically the whole process lasted less than 0.5 s. The scale bars represent 20 μm.

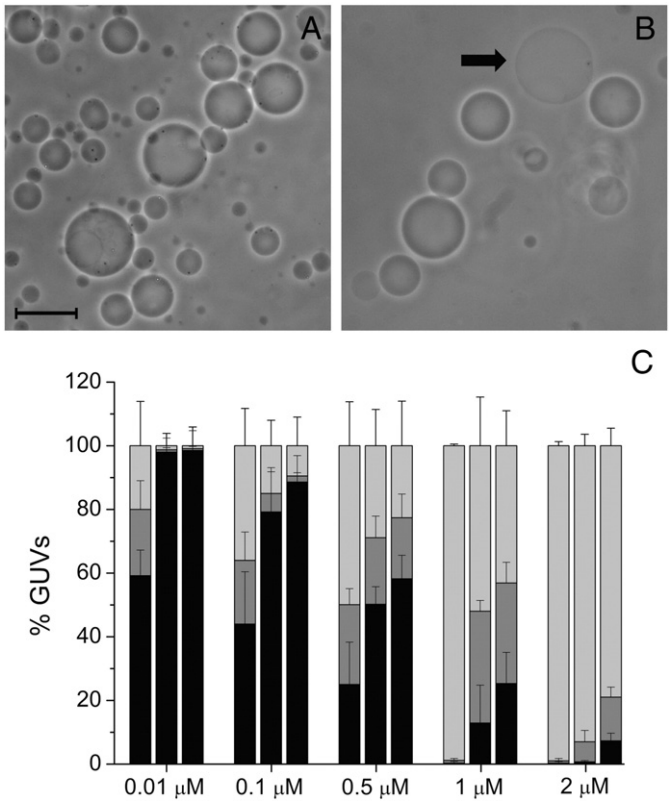

Fig. 8. Effects of CPPs on GUVs as seen by observing a vesicle population by phase contrast microscopy after 30 min of incubation. (A) Selected optical field captured with a medium magnification objective (20× Ph2), showing the usual disposition of GUVs due to gravity. (B) GUVs diluted in 0.5 μM PF3. The arrow points out a faded GUV (without phase contrast). The scale bar represents 100 μM. (C) Bars represent the percentages of intact (black), faded (dark gray) and burst (light gray) GUVs at 5 different CPP concentrations. The first bar at each concentration represents TP10, the second PF3 and the third PF6. The values represent the means and standard deviations for at least three independent experiments. In each experiment 216–384 vesicles were viewed.

concentration the fraction of intact vesicles decreased for all CPPs. TP10 exhibited the perforating effect already at 0.01 μM concentration, while comparable effects were observed with PF3 and PF6 at 0.5 μM concentration. The maximal effect (disintegration of all vesicles) was observed at the lowest concentration for TP10, in accord with the leakage study on LUVs. Thus stearylation decreases the ability of CPPs to induce leakage from vesicles, only becoming effective at higher concentrations. The similarity of the results obtained with PF3 and PF6 shows that the trifluoromethylquinoline moiety exerts little effect on GUV perforation.

4. Discussion

The PepFect family of cell-penetrating peptides was designed to increase the efficiency of cell-internalization and to overcome endosomal sequestration of applied CPP/nucleic acid complexes and thus to improve their transfection ability [33]. PF3 and PF6 are very effective for transfection *in vitro*, and PF6 also *in vivo*, but little is known about their effects on lipid membranes [10,11,34]. Since peptide/lipid interaction is essential for induction of a specific endocytotic pathway or membrane translocation we have evaluated the contribution of the stearyl and trifluoromethylquinoline moieties on the ability of CPPs to interact with lipid membranes by comparing the effects of TP10 with those of PF3 and PF3 with PF6, respectively.

Experiments at an air/water surface demonstrate that neither the stearyl nor the trifluoromethylquinoline moiety significantly influences the CMC. However, the stearyl moiety increases the affinity for a hydrophilic/hydrophobic interface (seen as a high π_{sat}) and the amphipathicity of the molecule (Fig. 2). According to its π_{sat} TP10 is a strong amphipathic peptide that contains alternating hydrophobic and cationic domains [35]. Since PF3 and PF6 contain the same peptide domain as TP10, the pronounced amphipathic character is a consequence of the increased hydrophobicity due to stearic acid modification. Hydrophobic domains are not essential for internalization, as proven for CPPs composed of polar residues like polyarginine and polylysine. Nevertheless, they promote hydrophobic interaction with membranes that are believed to play a key role, besides electrostatic interactions, for amphipathic CPPs [7]. Addition of hydrophobic fatty acyl moieties has been shown to promote cellular uptake [36–39]. Our experiments using the monolayer technique confirm insertion of stearylated peptides PF3 and PF6 into a lipid monolayer composed of zwitterionic phospholipids, with considerably higher MIPs than TP10 (Fig. 3). This is in agreement with the fact that MIP increases with the length of the fatty acid attached to the peptide surfactin [40]. Surprisingly, the addition of partly hydrophilic trifluoromethylquinoline moieties to the hydrophilic part of PF3, to give PF6 resulted in decreased amphipathicity, although this effect is rather small. The cellular membrane lateral pressure is estimated to be around 30–35 mN/m [19,41] and MIPs for TP10, PF3 and PF6 are higher. For this reason these CPPs are believed to insert spontaneously into the phospholipid monolayer and biological membranes [19]. The ability of TP10 to insert and interact with a lipid monolayer is considerably increased when the latter is composed of negatively charged POPG phospholipids, which indicates the large contribution of electrostatic interactions (Figs. 3A and 4). Structurally, TP10 resembles antimicrobial peptides that are able to discriminate between neutral (host-like) and negatively charged (target-like) membranes, and its ability to interact more strongly with partly negatively charged membranes has been demonstrated [26,42,43]. Since the presence of POPG does not improve peptide-lipid interaction, but rather slightly lowers MIPs for PF3 and PF6, hydrophobic interactions presumably play the key role in the modified CPPs-membrane interaction. All these results are corroborated also with the results obtained by SPR showing that the addition of acyl moiety to TP10 increased affinity for lipid monolayer, however, the effect being more pronounced with zwitterionic POPC than with anionic POPG (Fig. 4). Comparing the results obtained with PF3 and PF6 for the binding to lipid monolayer by different methods, the general conclusion is that the effect of the trifluoromethylquinoline moiety is very small or even negligible with the tendency to slightly decrease the affinity.

The membrane destabilizing and permeabilizing ability of CPPs was determined by observing GUVs by phase contrast microscopy and by measuring their ability to induce leakage in a lipid bilayer, using LUV and GUV membrane mimetic systems. It was shown (see Results and Fig. 7) that all three tested CPPs destabilize the membrane of GUVs. Growth and shape transformation of GUVs have already been observed in different experimental systems studying the interaction of vesicles with peptides [31], proteins [44] and lipids [45]. These phenomena seem to be related to the intercalation of agent into the membrane and the modification of the membrane curvature [44]. For the cell-internalization of CPP the destabilization of the membrane could be of relevance since it could provide facilitated passage of CPP and cargo through the membrane. Additionally, it could help membrane to reorganize what is an important step in different mechanisms of endocytosis.

We also showed that TP10 is very potent membrane leakage inducer in LUVs and GUVs. As observed with POPC in both systems, stearylation reduces the leakage induction of PF3 and PF6, while the addition of trifluoromethylquinoline moieties to the peptide does not have a major effect on the pore formation (Fig. 5A). The effect of stearylation seems surprising if we compare PF3 and PF6 with acylated cationic antimicrobial peptides which show better membrane binding ability as their non-acylated parent peptides, and, in general, also more pronounced leakage activity [46]. This contradiction, on

one hand, might result from the length of the acyl tail for which it was shown to affect differentially the pore formation of the acylated antimicrobial peptides [47]. Acyl tail in lipidated antimicrobial peptides was in all known cases shorter than in the case of PF3 and PF6. On the other hand, it was also found that in some cases lipidation of peptides does not in itself favors permeabilization but can make it less efficient, depending on the structure of peptide moiety and membrane lipid composition [47]. It seems possible, that the acylation can partly block pore formation by restricting peptide thus preventing the reorganization within the membrane that leads to the pore formation. As it was observed, the leakage of LUVs induced by TP10, PF3 and PF6, is the result of the formation of pore-like structures rather than the degradation of vesicles (Fig. 6). Additional structural studies of PepFect peptides including the variable length of the lipid tail are planned to clarify these open questions. In accordance with penetration experiments, the addition of POPG to LUV membranes reduces the leakage induced by PF3 and PF6 (Fig. 5B). This shows stronger interaction of TP10 with anionic than with zwitterionic lipids but in spite of this it is a less potent leakage inducer in POPC:POPG LUVs than in pure POPC LUVs (Fig. 5B). A plausible explanation is that, in a net negatively charged membrane, electrostatic forces retain positively charged TP10 molecules in the headgroup region, while in zwitterionic membrane it can insert deeply and lead to major disturbance of the bilayer [42]. The acylation of TP10 introduces more hydrophobic nature to the peptide and obviously increases the affinity for zwitterionic membranes. In the case of smaller peptides its hydrophobic nature prevails even upon further hydrophilic modification with the trifluoromethylquinoline moieties, as observed here by the similar properties of PF3 and PF6.

Trifluoromethylquinoline moiety has been shown to have very small effects on all studied processes. Without knowing the exact impact of this moiety on the peptide structure and its hydrophobicity it is hard to understand our results. Trifluoromethylquinoline moiety is mainly not charged at the used pH of 7.5 ($pKa1 = 7.8$; $pKa2 = 9.7$; [48]) but it incorporates several nitrogen atoms that can form hydrogen bonds with water and hydrophobic ring structures, therefore, it is itself moderately amphipathic. It seems, however, that in spite of relatively large dimensions the moiety does not change general properties of peptide, possibly because of the similarity in amphipathicity. However, it promotes aggregation of PF6 (Fig. 6D), but also with PF6 in the aggregated state we have not detected any differences in membrane binding and pore formation.

Our study does not cover the impact of the structure of tested CPPs but we are aware that the interaction of peptides with the membrane strongly depends on peptide secondary structure, as it was shown for several CPPs [24] and related antimicrobial peptides [46]. It is well known that both types of these peptides are mainly non-structured in solution but they usually acquire at least in part α-helical or, in some cases, β-sheet structure. This is true also for TP10 for which it was shown that α-helical structure is associated with strong CPP–membrane interaction [26]. Similar studies with acylated analogs of TP10 have not been found in the literature and the effect of the acyl tail on the structure of TP10 is not known. Studies of acylated cationic antimicrobial peptides that share many structural features with acylated TP10 have revealed that acylation with long fatty acid promote the formation of α-helical secondary structure and increase the interaction with lipid membrane [46]. This is in accordance with our observations that PF3 and PF6 more strongly interact with the membrane than TP10 (see Figs. 3 and 4) and might indicate greater inclination of PF3 and PF6 to fold in α-helix than TP10.

In conclusion, we have shown that the addition of a stearyl moiety to TP10 increases the amphipathicity of the peptide and improves the insertion of CPPs into a lipid monolayer composed of zwitterionic lipids. However, it decreases leakage, and hence pore formation, in the LUV and GUV membrane mimetic systems, which seems to be the cause of lower toxicity of PF3 and PF6 in comparison to TP10. The trifluoromethylquinoline moiety does not exert much influence on CPP interaction with a lipid membrane and it does not interfere with pore formation, while it induces the aggregation of PF6 molecules. However, aggregation does not modify the interaction of PF6 with lipids. This shows that endosomal escape is not the consequence of the modified interaction of peptide with lipid bilayer but is the result of other processes, for instance the osmotic swelling of endosome by increase of its pH after binding of protons to trifluoromethylquinoline, as already suggested. The presence of negatively charged phospholipids in the membrane improves the peptide/lipid monolayer interaction for TP10 and decreases the interaction in the case of PF3 and PF6. This indicates the importance of electrostatic interactions in binding to the membrane in the case of TP10 and hydrophobic interactions in the case of PF3 and PF6 and also shows differences in affinity of PepFect CPPs for various types of lipids. This selectivity could explain the ability of PF3 and PF6 to cluster lipids in membrane bilayer [5] and together with the shown propensity for the destabilization of the membrane it could contribute to the cell-penetration ability of PF3 and PF6.

Acknowledgements

We thank Vesna Arrigler for preparing GUVs and Vesna Hodnik for help with SPR. The work was supported by the Slovenian Research Agency, the Swedish Research Council (VR-NT), the Center for Biomembrane Research, Stockholm and the Sweden–Japan research project.

References

[1] M. Lindgren, Ü. Langel, Classes and prediction of cell-penetrating peptides, Methods Mol. Biol. 683 (2011) 3–19.
[2] M. Zorko, Ü. Langel, Cell-penetrating peptides: mechanism and kinetics of cargo delivery, Adv. Drug Deliv. Rev. 57 (2005) 529–545.
[3] H. Räägel, P. Säälik, M. Pooga, Peptide-mediated protein delivery—which pathways are penetrable? Biochim. Biophys. Acta 1798 (2010) 2240–2248.
[4] F. Heitz, M.C. Morris, G. Divita, Twenty years of cell-penetrating peptides: from molecular mechanisms to therapeutics, Br. J. Pharmacol. 157 (2009) 195–206.
[5] P. Säälik, A. Niinep, J. Pae, M. Hansen, D. Lubenets, Ü. Langel, M. Pooga, Penetration without cells: membrane translocation of cell-penetrating peptides in the model giant plasma membrane vesicles, J. Control. Release 153 (2011) 117–125.
[6] M. Hansen, E. Eriste, Ü. Langel, The internalization mechanisms and bioactivity of the cell-penetrating peptides, in: B. Groner (Ed.), Peptides as Drugs: Discovery and Development, John Wiley and Sons, Weinheim, 2009, pp. 221–234.
[7] S. Pujals, J. Fernandez-Carneado, C. Lopez-Iglesias, M.J. Kogan, E. Giralt, Mechanistic aspects of CPP-mediated intracellular drug delivery: relevance of CPP self-assembly, Biochim. Biophys. Acta 1758 (2006) 264–279.
[8] J.S. Wadia, R.V. Stan, S.F. Dowdy, Transducible TAT-HA fusogenic peptide enhances escape of TAT-fusion proteins after lipid raft macropinocytosis, Nat. Med. 10 (2004) 310–315.
[9] P. Lundberg, S. El-Andaloussi, T. Sütlü, H. Johansson, Ü. Langel, Delivery of short interfering RNA using endosomolytic cell-penetrating peptides, FASEB J. 21 (2007) 2664–2671.
[10] M. Mäe, S. El Andaloussi, P. Lundin, N. Oskolkov, H.J. Johansson, P. Guterstam, Ü. Langel, A stearylated CPP for delivery of splice correcting oligonucleotides using a non-covalent co-incubation strategy, J. Control. Release 134 (2009) 221–227.
[11] S. El Andaloussi, T. Lehto, I. Mäger, K. Rosenthal-Aizman, I.I. Oprea, O.E. Simonson, H. Sork, K. Ezzat, D.M. Copolovici, K. Kurrikoff, J.R. Viola, E.M. Zaghloul, R. Sillard, H.J. Johansson, F. Said Hassane, P. Guterstam, J. Suhorutsenko, P.M. Moreno, N. Oskolkov, J. Hälldin, U. Tedebark, A. Metspalu, B. Lebleu, J. Lehtio, C.I. Smith, Ü. Langel, Design of a peptide-based vector, PepFect6, for efficient delivery of siRNA in cell culture and systemically *in vivo*, Nucleic Acids Res. 39 (2011) 3972–3987.
[12] U. Soomets, M. Lindgren, X. Gallet, M. Hallbrink, A. Elmquist, L. Balaspiri, M. Zorko, M. Pooga, R. Brasseur, Ü. Langel, Deletion analogues of transportan, Biochim. Biophys. Acta 1467 (2000) 165–176.
[13] M. Avbelj, S. Horvat, R. Jerala, The role of intermediary domain of MyD88 in cell activation and therapeutic inhibition of TLRs, J. Immunol. 187 (2011) 2394–2404.
[14] J. Cheng, R. Zeidan, S. Mishra, A. Liu, S.H. Pun, R.P. Kulkarni, G.S. Jensen, N.C. Bellocq, M.E. Davis, Structure–function correlation of chloroquine and analogues as transgene expression enhancers in nonviral gene delivery, J. Med. Chem. 49 (2006) 6522–6531.
[15] R. Marches, J.W. Uhr, Enhancement of the p27Kip1-mediated antiproliferative effect of trastuzumab (Herceptin) on HER2-overexpressing tumor cells, Int. J. Cancer 112 (3) (2004) 492–501.

[16] S. El-Andaloussi, P. Jarver, H.J. Johansson, Ü. Langel, Cargo-dependent cytotoxicity and delivery efficacy of cell-penetrating peptides: a comparative study, Biochem. J. 407 (2007) 285–292.
[17] S. Deshayes, K. Konate, G. Aldrian, F. Heitz, G. Divita, Interactions of amphipathic CPPs with model membranes, Methods Mol. Biol. 683 (2011) 41–56.
[18] R. Maget-Dana, The monolayer technique: a potent tool for studying the interfacial properties of antimicrobial and membrane-lytic peptides and their interactions with lipid membranes, Biochim. Biophys. Acta 1462 (1999) 109–140.
[19] P. Calvez, S. Bussieres, D. Eric, C. Salesse, Parameters modulating the maximum insertion pressure of proteins and peptides in lipid monolayers, Biochimie 91 (2009) 718–733.
[20] M.I. Angelova, S. Soleau, P. Meleard, J.F. Faucon, P. Bothorel, Preparation of giant vesicles by external AC electric fields. Kinetics and applications, Colloid Polym. Sci. 192 (1992) 127–131.
[21] M. Mally, J. Majhenc, S. Svetina, B. Zeks, The response of giant phospholipid vesicles to pore-forming peptide melittin, Biochim. Biophys. Acta 1768 (2007) 1179–1189.
[22] H. Mozsolits, H.J. Wirth, J. Werkmeister, M.I. Aguilar, Analysis of antimicrobial peptide interactions with hybrid bilayer membrane systems using surface plasmon resonance, Biochim. Biophys. Acta 1512 (2001) 64–76.
[23] M.A. Cooper, A.C. Try, J. Carroll, D.J. Ellar, D.H. Williams, Surface plasmon resonance analysis at a supported lipid monolayer, Biochim. Biophys. Acta 1373 (1998) 101–111.
[24] M. Beseničar, P. Maček, J.H. Lakey, G. Anderluh, Surface plasmon resonance in protein–membrane interactions, Chem. Phys. Lipids 141 (2006) 169–178.
[25] C. Urban, P. Schurtenberger, Characterization of turbid colloidal suspensions using light scattering techniques combined with cross-correlation methods, J. Colloid Interface Sci. 207 (1998) 150–158.
[26] E. Eiriksdottir, K. Konate, Ü. Langel, G. Divita, S. Deshayes, Secondary structure of cell-penetrating peptides controls membrane interaction and insertion, Biochim. Biophys. Acta 1798 (2010) 1119–1128.
[27] D. Attwood, A.D. Florence, Surfactant Systems: Their Chemistry, Pharmacy and Biology, Chapmann and Hall, London, 1984.
[28] R. Verger, F. Pattus, Lipid–protein interactions in monolayers, Chem. Phys. Lipids 30 (1982) 189–227.
[29] Q. Hong, I. Gutierrez-Aguirre, A. Barlič, P. Malovrh, K. Kristan, Z. Podlesek, P. Maček, D. Turk, J.M. Gonzalez-Manas, J.H. Lakey, G. Anderluh, Two-step membrane binding by Equinatoxin II, a pore-forming toxin from the sea anemone, involves an exposed aromatic cluster and a flexible helix, J. Biol. Chem. 277 (2002) 41916–41924.
[30] F. Madani, A. Peralvarez-Marin, A. Gräslund, Liposome model systems to study the endosomal escape of cell-penetrating peptides: transport across phospholipid membranes induced by a proton gradient, J. Drug Deliv. (2011), doi: 10.1155/2011/897592.
[31] M. Mally, J. Majhenc, S. Svetina, B. Zeks, Mechanisms of equinatoxin II-induced transport through the membrane of a giant phospholipid vesicle, Biophys. J. 83 (2002) 944–953.
[32] J. Majhenc, S. Svetina, M. Zorko, B. Žekš, Lipid-polypeptide interactions studied by optical observation of a single giant lipid vesicle, in: A. Pramanik (Ed.), Biochemistry and Biophysics of Lipids, Transworld Research Network, Kerala, 2006, p. 192.
[33] S. El Andaloussi, T. Lehto, P. Lundin, Ü. Langel, Application of PepFect peptides for the delivery of splice-correcting oligonucleotides, Methods Mol. Biol. 683 (2011) 361–373.
[34] F.S. Hassane, R. Abes, S. El Andaloussi, T. Lehto, R. Sillard, Ü. Langel, B. Lebleu, Insights into the cellular trafficking of splice redirecting oligonucleotides complexed with chemically modified cell-penetrating peptides, J. Control. Release 153 (2011) 163–172.
[35] A. Ziegler, Thermodynamic studies and binding mechanisms of cell-penetrating peptides with lipids and glycosaminoglycans, Adv. Drug Deliv. Rev. 60 (2008) 580–597.
[36] I.A. Khalil, S. Futaki, M. Niwa, Y. Baba, N. Kaji, H. Kamiya, H. Harashima, Mechanism of improved gene transfer by the N-terminal stearylation of octaarginine: enhanced cellular association by hydrophobic core formation, Gene Ther. 11 (2004) 636–644.
[37] J. Fernandez-Carneado, M.J. Kogan, N. Van Mau, S. Pujals, C. Lopez-Iglesias, F. Heitz, E. Giralt, Fatty acyl moieties: improving Pro-rich peptide uptake inside HeLa cells, J. Pept. Res. 65 (2005) 580–590.
[38] A.R. Nelson, L. Borland, N.L. Allbritton, C.E. Sims, Myristoyl-based transport of peptides into living cells, Biochemistry 46 (2007) 14771–14781.
[39] T. Lehto, R. Abes, N. Oskolkov, J. Suhorutsenko, D.M. Copolovici, I. Mäger, J.R. Viola, O.E. Simonson, K. Ezzat, P. Guterstam, E. Eriste, C.I. Smith, B. Lebleu, S. El Andaloussi, Ü. Langel, Delivery of nucleic acids with a stearylated (RxR)4 peptide using a non-covalent co-incubation strategy, J. Control. Release 141 (2010) 42–51.
[40] M. Eeman, A. Berquand, Y.F. Dufrene, M. Paquot, S. Dufour, M. Deleu, Penetration of surfactin into phospholipid monolayers: nanoscale interfacial organization, Langmuir 22 (2006) 11337–11345.
[41] D. Marsh, Intrinsic curvature in normal and inverted lipid structures and in membranes, Biophys. J. 70 (1996) 2248–2255.
[42] E. Barany-Wallje, J. Gaur, P. Lundberg, Ü. Langel, A. Gräslund, Differential membrane perturbation caused by the cell penetrating peptide Tp10 depending on attached cargo, FEBS Lett. 581 (2007) 2389–2393.
[43] L.E. Yandek, A. Pokorny, A. Florén, K. Knoelke, Ü. Langel, P.F. Almeida, Mechanism of the cell-penetrating peptide transportan 10 permeation of lipid bilayers, Biophys. J. 92 (2007) 2434–2444.
[44] T. Baumgart, B.R. Capraro, C. Zhu, S.L. Das, Thermodynamics and mechanics of membrane curvature generation and sensing by proteins and lipids, Annu. Rev. Phys. Chem. 62 (2011) 483–506.
[45] P. Peterlin, V. Arrigler, K. Kogej, S. Svetina, P. Walde, Growth and shape transformations of giant phospholipid vesicles upon interaction with an aqueous oleic acid suspension, Chem. Phys. Lipids 159 (2009) 67–76.
[46] S.K. Straus, R.E.W. Hancock, Mode of action of new antibiotic for Gram-positive pathogens daptomycin: comparison with cationic antimicrobial peptides and lipopeptides, Biochim. Biophys. Acta 1758 (2006) 1215–1223.
[47] B. Vad, L.A. Thomsen, K. Bertelsen, M. Franzmann, J.M. Pedersen, S.B. Nielsen, T. Vosegaard, Z. Valnickova, T. Skrydstrup, J.J. Enghild, R. Wimmer, N.C. Nielsen, D.E. Otzen, Divorcing folding from function: how acylation affects the membrane-perturbing properties of an antimicrobial peptide, Biochim. Biophys. Acta 1804 (2010) 806–820.
[48] A. Krasowska, L. Chmielewska, J. Łuczyński, S. Witek, K. Sigler, The dual mechanism of the antifungal effect of new lysosomotropic agents on the *Saccharomyces cerevisiae* RXII strain, Cell. Mol. Biol. Lett. 8 (2003) 111–120.